

SUPPLEMENTAL INFORMATION

Energy flux densities near the electron dissipation region in asymmetric magnetopause reconnection

J. P. Eastwood^{1,*}, M. V. Goldman², T. D. Phan³, J. E. Stawarz¹, P. A. Cassak⁴, J. F. Drake⁵, D. Newman², B. Lavraud⁶, M. A. Shay⁷, R. E. Ergun⁸, J. L. Burch⁹, D. J. Gershman¹⁰, B. L. Giles¹⁰, P. A. Lindqvist¹¹, R. B. Torbert^{12,9}, R. J. Strangeway¹³ and C. T. Russell¹³

¹*The Blackett Laboratory, Imperial College London, London SW7 2AZ, UK*

²*Department of Physics, University of Colorado, Boulder, Colorado 80303, USA*

³*Space Sciences Laboratory, University of California, Berkeley, California 94720, USA*

⁴*Department of Physics and Astronomy and Centre for KINETIC Plasma Physics, West Virginia University, Morgantown, West Virginia 26506, USA*

⁵*Department of Physics/Institute for Physical Science and Technology, University of Maryland College Park, Maryland 20742, USA*

⁶*Institut de Recherche en Astrophysique et Planétologie, CNRS, UPS, CNES, Université de Toulouse, Toulouse, France*

⁷*Department of Physics and Astronomy, University of Delaware, Newark, Delaware 19716, USA*

⁸*LASP/Department of Astrophysical and Planetary Sciences, University of Colorado, Boulder, Colorado 80303, USA*

⁹*Southwest Research Institute, San Antonio, Texas 78238, USA*

¹⁰*NASA, Goddard Space Flight Center, Greenbelt, Maryland 20771, USA*

¹¹*KTH Royal Institute of Technology, Stockholm, Sweden*

¹²*University of New Hampshire, Durham, New Hampshire 03824, USA*

¹³*Institute of Geophysics, Earth, Planetary, and Space Sciences, University of California, Los Angeles, Los Angeles, California 90095, USA*

For context, variations in \mathbf{Q}_i and \mathbf{Q}_e and \mathbf{S} can be compared to the total energy density [8] of each species

$$U_s = U_{s,kinetic} + U_{s,thermal} = \frac{1}{2} m_s n_s v_s^2 + \frac{Tr(\overline{\mathbf{P}}_s)}{2},$$

and the electromagnetic energy density

$$U_{EM} = \frac{1}{2} \epsilon_0 E^2 + \frac{1}{2} \frac{B^2}{\mu_0},$$

as shown in figure S1. While it is difficult to distinguish temporal evolution from spatial dependence in satellite observations, we include this information as a way to gain insight to where spatial changes in flux densities may lead to temporal evolution of energy density.

U_i (Figure S1e) is largest at the beginning and end of the interval where the exhaust is fastest. At the beginning of the interval there is an approximately equal split between the ion kinetic and thermal energy density whereas at the end of the interval, the ion thermal energy is higher. The ion kinetic energy density is not negligible and this is consistent with previous observations [Eastwood et al., 2013; Yamada et al., 2014]. In contrast, U_e (Figure S1g) is almost entirely thermal, and an order of magnitude smaller than U_i . The dominance of the thermal component in U_e is to be expected given the small particle mass and the high electron thermal speeds typically observed in space plasmas. The MMS data also reveals more structure compared to the ions, and is locally enhanced both in the region surrounding the EDR and also after the separatrix encounter at 13:06:59 UT, with two other peaks around 13:07:01 UT. The electromagnetic energy density U_{EM} (Figure S1i) essentially follows $|B|^2$, and is peaked at the separatrix region, where S is also enhanced. It also peaks adjacent to the EDR encounter with further structure in between. The peaks in U_{EM} are adjacent to the increases in electron energy density. After the EDR encounter, the electromagnetic energy density is reduced but MMS remained closer to the midplane at smaller values of B_L , away from the separatrix region.

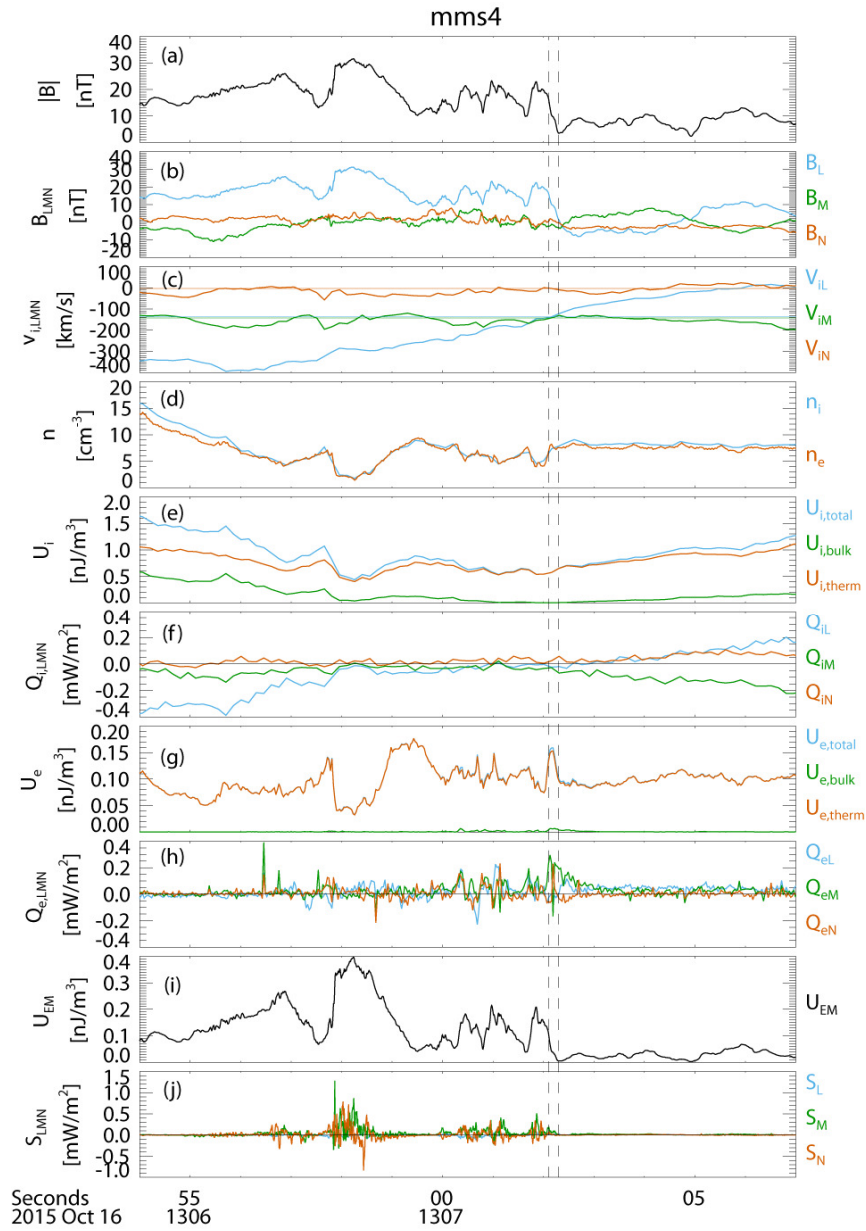


Figure S1 (a-b) magnetic field strength and components (c) ion velocity (d) number density (e-f) ion energy density and energy flux (g-h) electron energy density and energy flux (i-j) electromagnetic energy density and energy flux.